JOURNAL OF VIROLOGY, Jan. 1993, p. 119–130
0022-538X/93/010119-12$02.00/0

Vol. 67, No. 1

Role of Nuclear Pore Complex in Simian Virus 40 Nuclear Targeting

MASAYASU YAMADA AND HARUMI KASAMATSU*

Department of Biology and Molecular Biology Institute, University of California, Los Angeles, 405 Hilgard Avenue, Los Angeles, California 90024

Received 28 May 1992/Accepted 30 September 1992

Cytoplasmically injected simian virus 40 (SV40) virions enter the nucleus through nuclear pore complexes (NPCs) and can express large T antigen shortly thereafter (J. Clever, M. Yamada, and H. Kasamatsu, Proc. Natl. Acad. Sci. USA 88:7333–7337, 1991). The nuclear import of the protein components of introduced SV40 was reversibly arrested by chilling and energy depletion, corroborating our previous observation that the nuclear entry of injected SV40 is blocked in the presence of wheat germ agglutinin and an antinucleoporin monoclonal antibody (mAb414), general inhibitors of NPC-mediated import. The nuclear accumulation of virion protein components and large T antigen in nonpermissive NIH 3T3 cells was similar to that in the permissive host, indicating that the ability to use NPCs as a route of nuclear entry appears to be a general property of the injected virus. Injected virions were capable of completing their lytic cycle and forming plaques in permissive cells. During the early phase of SV40 infection, the cytoplasmic injection of mAb414 effectively blocked nuclear T-antigen accumulation for up to 8 h of infection but had very little effect after 12 h of infection. The time-dependent interference with nuclear T-antigen accumulation by the antinucleoporin antibody is consistent with the hypothesis that the infecting virions enter the nucleus through NPCs. The interference study also suggests that the early phase of infection consists of at least two steps: a step for virion cell entry and intracytoplasmic trafficking and a step for virion nuclear entry followed by large-T-antigen gene expression and subsequent nuclear localization of the gene product. Virions were visualized as electron-dense particles in ultrathin sections of samples in which transport was permitted or arrested. In the former cells, electron-dense particles were predominantly observed in the nucleus. The virions were distributed randomly and nonuniformly in the nucleoplasm but were not observed in heterochromatin or in nucleoli. In the latter cells, the electron-dense particles were seen intersecting the nuclear envelope, near the inner nuclear membrane, and in NPCs. In tangential cross sections of NPCs, which appeared as donut-shaped structures, a spherical electron-dense particle was observed in the center of the structure. Immunoelectron microscopy revealed that NPCs were selectively decorated with 5-nm colloidal gold particles–anti-Vp1 immunoglobulin G at the cytoplasmic entrance to and in NPCs, confirming that the morphologically observed electron-dense particles in NPCs contain the viral structural protein. These results support the hypothesis that the nuclear import of SV40 is catalyzed through NPCs by an active transport mechanism that is similar to that of other karyophiles.

Animal viruses utilize unique subcellular sites for their multiplication. Information necessary for targeting infectious virions to their reproductive site in the cell is contained within the virion structural proteins (15). For papovaviruses, a family of DNA tumor viruses including murine polyomavirus, simian virus 40 (SV40), and human BK and JC viruses, all viral multiplication processes, genome replication, nucleocapsid formation, and progeny virion maturation in a permissive host, as well as integration of the viral genome into host chromosomes in nonpermissive hosts, occur in the nucleus (41). Thus, the targeting of an infectious particle to the nucleus following its entrance into both permissive and nonpermissive host cells is a key event in the virion life cycle. Early stages of infection include the epitope-specific binding of virion particles to the cell surface, internalization of the particles into the cytoplasm, and release of viral DNA from the virion coat in the nucleus (15, 41). In reported studies, virions have been observed in various cytoplasmic organelles, including mitochondria, lysosomes, the endoplasmic reticulum, and the Golgi apparatus (23, 25, 30, 32). Internalization of electron-dense particles into the intracisternal space of the nuclear envelope also has been reported (23, 25, 30, 32). A postulated route for virion nuclear entry involves fusion of the plasma membrane containing endocytosed virions with the outer nuclear membrane, thereby releasing into the perinuclear cisterna the virions, which subsequently enter the nucleus through the inner nuclear membrane by an unknown mechanism (22, 23, 25, 30, 32, 35). We showed that the nuclear import of virion particles introduced directly into the cytoplasm by injection was sensitive to inhibitors of nuclear pore complex (NPC)-mediated transport and that these particles were competent for large-T-antigen expression (9). The protein components of introduced virions, as well as electron-dense virion particles, accumulated in the nucleus within 1 to 2 h after cytoplasmic injection, and an early gene product, large T antigen, accumulated in the nucleus 3 h after cytoplasmic injection. Thus, the introduction of virions directly into the cytoplasm shortened the duration required for the onset of large-T-antigen expression in SV40-infected cells. The nuclear accumulation of virion proteins and large T antigen was blocked by coinjection of virions with NPC-inhibitory reagents, such as lectin wheat germ agglutinin or an antinucleoporin monoclonal antibody, mAb414. In ultrathin sections of the mAb414-coinjected cells, electron-dense particles

* Corresponding author.

were predominantly observed in the cytoplasm and in the vicinity of the nuclear envelope. These observations are consistent with the idea that an injected SV40 particle can enter the nucleus through an NPC by a mediated transport mechanism, as has been shown for karyophilic proteins (7, 10, 13). This NPC-mediated nuclear entry route of injected virions is in contrast to the fusion-driven nuclear entry route postulated to occur during infection. While our approach, delivering virions directly to the cytoplasm, abbreviates the cell entry process(s) of infecting virions, the first step of infection, it may elucidate ambiguous steps pertaining to the early phase of infection.

NPCs are large, highly symmetrical structures that join at intervals the outer and inner nuclear membranes of the nuclear envelope (3, 17, 38, 42). They provide aqueous channels, allowing the diffusion of small molecules but restricting the passage of large macromolecules unless the signal-responsive gating process allows their passage (6, 27, 28, 36, 37). The nuclear entry of karyophilic proteins through NPCs is dependent on a nuclear localization signal (NLS) and is an active process (7, 10, 13, 33, 39). The selective transport process is divided into at least two steps: NLS-dependent binding to the nuclear envelope, presumably to the transporter in an energy-independent manner, and translocation through the NPC. The latter step is temperature and energy dependent (7, 33, 39) and is arrested by chilling, by depletion of metabolic energy, or by the addition of wheat germ agglutinin, which binds to *N*-acetylglucosamine and sialic acid, or antibodies that recognize a subset of nucleoporins, a family of NPC proteins (11, 16, 44). The binding sites for wheat germ agglutinin, mAb414, and an NPC-transported protein, nucleoplasmin, have been mapped to the central region of NPCs (4), which has been shown to be the site of protein translocation and hence has been named the central transporter (4).

In this study, we have tested whether virion nuclear entry is arrested by chilling or energy depletion, whether virions are effectively targeted to the nucleus of nonpermissive cells (NIH 3T3), and whether cytoplasmically injected virions are capable of completing the infectious cycle. We have also studied a possible role of NPCs in SV40 infection. Ultrastructural evidence for the presence of SV40 in NPCs is also presented to further support our conclusion that SV40 particles can enter the nucleus through NPCs. The localization of virion particles was further ascertained by immunoelectron microscopy with anti-Vp1 immunoglobulin G (IgG).

MATERIALS AND METHODS

Cells and viruses. TC7 cells, a subline of the African green monkey kidney epitheloid cell line, and NIH 3T3 cells were maintained and passaged in TC7 cell medium which is Dulbecco's modified Eagle's medium supplemented with arginine hydrochloride (0.3 mg/ml), glutamine (1.5 mg/ml), histidine hydrochloride (20 μg/μl), glucose (5 mg/ml), and 10% fetal bovine serum.

The purification of SV40 virions was performed as previously described (26), and virion stock preparations (8×10^{14} to 10×10^{14} physical particles per ml) were stored at −20°C in CsCl (1.34 g/ml) containing *N*-2-hydroxyethylpiperazine-*N'*-2-ethanesulfonic acid (HEPES)-buffered saline (25 mM HEPES [pH 7.2], 137 mM NaCl, 5 mM KCl, 0.8 mM Na_2HPO_4) (CsCl–HEPES-buffered saline).

Microinfection and microinjection. SV40 virion particles in CsCl–HEPES-buffered saline were used to microinfect the apical surface of TC7 cell monolayers or were microinjected into the cell cytoplasm as previously described (8, 9). For virion neutralization, 0.3 ml of calf anti-SV40 serum (Flow Laboratories, McLean, Va.) was added to 6 ml of culture medium during microinjection. For TC7 cells, the virion stock solution was diluted with CsCl–HEPES-buffered saline to 10^{14} physical particles per ml. The number of virion particles injected into the cytoplasm was varied from 10^3 to 10^4 particles per cell and was sufficient to detect both major Vp1 and minor Vp2 and Vp3 proteins. In some experiments, 10 to 100 particles per cell were cytoplasmically injected. CsCl was included for convenience but was not essential for aimed microinjection. A virion stock solution in HEPES-buffered saline was just as effective as one in CsCl–HEPES-buffered saline (data not shown). For microinjection of NIH 3T3 cells, the virion stock solution was diluted with HEPES-buffered saline without CsCl. NIH 3T3 cells were much more sensitive to hypertonicity than TC7 cells, and the presence of 0.3 M CsCl resulted in cell death following cytoplasmic microinjection. For electron microscopy (EM) studies, the injected cells or infected cells were marked as an islet by scraping with a glass microcapillary surrounding cells and then cultured in 10% fetal bovine serum-containing TC7 cell medium. In some experiments, the virion particles were comicroinjected with antinucleoporin monoclonal antibody mAb414 (1 mg/ml).

Indirect immunofluorescence. Hamster anti-large-T-antigen polyclonal antibody, rabbit anti-Vp1 antibody, guinea pig anti-Vp1 antibody, rabbit anti-Vp3 antibody, and antinucleoporin monoclonal antibody mAb414 were previously described (9). Rabbit anti-Vp3 antibody recognizes both Vp2 and Vp3 of SV40 (29). Fluorescein isothiocyanate (FITC)–goat anti-rabbit IgG, FITC–goat anti-hamster IgG, tetramethylrhodamine isothiocyanate (TRITC)–goat anti-guinea pig IgG, TRITC–goat anti-rabbit IgG, or TRITC–goat anti-mouse IgG were from Oregon-Teknika-Cappel (Cochranville, Pa.). Cells were grown on glass coverslips etched with a diamond pen to facilitate localization of the site for microinfection or microinjection. At various times after microinfection or microinjection, the cells were washed with ice-cold Dulbecco's phosphate-buffered saline (PBS) and fixed with 2% paraformaldehyde in PBS for 5 min at room temperature. The cells were washed with PBS, permeabilized with absolute methanol at −20°C, incubated with the primary antibody at a 1:40 dilution for 45 min at room temperature, rinsed thoroughly, and then incubated for 45 min with a 1:100 dilution of a fluorescence-labeled secondary antibody. Finally, the coverslips were mounted in Gelvatol and viewed and photographed on a fluorescence microscope (8).

Chilling and energy depletion studies. For the temperature arrest experiment, cells that had been precooled on ice for 1 h were cytoplasmically microinjected with SV40 particles and then incubated for 2 h on ice before fixation. For the temperature reversal experiment, the microinjected cells, after incubation on ice, were shifted to 37°C for 1 h before fixation. For glucose depletion experiments, cells were preincubated for 1 h at 37°C in glucose-free Eagle's basal medium supplemented with 10% dialyzed newborn calf serum in the presence or absence of 6 mM 2-deoxyglucose and 10 mM sodium azide. After cytoplasmic microinjection, cells were incubated in the same medium at 37°C for 2 h before fixation. For the reversal experiment, energy-depleted microinjected cells were transferred to Eagle's basal medium with 10% newborn calf serum for additional incubation at 37°C for 1 h.

Plaque assay. Cells were plated 1 day prior to injection or

infection on a 60-mm plastic culture dish in the bottom of which 2-mm circles had been etched. The cells inside the circles were microinfected or cytoplasmically microinjected with SV40 particles in the presence or absence of SV40-neutralizing antiserum. Following microinfection or microinjection, cells were cultured for 1 h in the presence or absence of the neutralizing antiserum in TC7 cell medium. They were then washed with TD buffer (9), overlaid with 3 ml of 0.8% soft agar–Eagle's minimum essential medium containing 5% fetal bovine serum, and incubated for 7 days. On the 7th day, these cells received a second overlay and were incubated for an additional 7 days. For the visualization of plaques, cells were fixed with 3.7% formaldehyde in PBS for 5 min after the agar medium had been carefully loosened from the plate at the edges and removed by inversion; cells were then washed with PBS and stained with 1% crystal violet (14).

Microinjection of antinucleoporin monoclonal antibody mAb414 into SV40-microinfected cells. A total of about 100 cells on either of the two sides of an etched line on a coverslip were microinfected with SV40 (10^{14} physical particles per ml) in CsCl–HEPES-buffered saline. The marked line was brought into the center of the viewing field of the eyepiece, and mAb414 (1 mg/ml) or the mouse antihuman kappa chain-constant-region antibody Idh 3.3.6 (1 mg/ml) was cytoplasmically injected into the cells on one side of the line 1, 4, 8, or 12 h after microinfection. Twenty hours after microinfection, the cells were fixed and then immunocytochemically stained as described above for the detection of nuclear large T antigen and mouse monoclonal antibody mAb414.

EM. Samples for EM were fixed in 2.5% glutaraldehyde in Dulbecco's PBS for 1 h at room temperature and kept in 1% glutaraldehyde overnight or until EM processing. For EM processing, the monolayers were washed three times with 50 mM Na cacodylate buffer (pH 7.3), fixed with 1% osmium tetroxide for 30 min in the dark, rinsed with distilled water, stained overnight at 4°C with fresh aqueous 1% uranyl acetate, dehydrated in an ethanol series (60 to 100%) with propylene oxide, and embedded flat in Epon 812. Coverslips were removed by liquid N_2 immersion. Marked cells were visible following toluidine blue staining, and the marked area, ranging from 1 to 2 mm^2, was selectively trimmed with a razor blade. Thin sections of 600 to 1,000 Å (60 to 100 nm) were made with a Sorvall MT-1 ultramicrotome, mounted on Parlodion-coated and carbon-stabilized copper grids, stained with uranyl acetate and then with Reynold's lead citrate, and viewed on a Philips 410 EM at 120 keV. The substratum cell attachment side could be oriented within a section, as it faced the Epon surface. For serial sections, sections were made as parallel as possible but oblique to the plane of the Epon surface, allowing identification of cells relative to the substratum side. Measurements of the diameters of virion particles and NPCs and the distance between NPCs were performed on photographs enlarged to a magnification of ×200,000. The number of virions in the nucleoplasm of the cells in which transport was permitted, 2.5 virion particles per μm^2, was obtained by counting the number of distinct electron-dense particles in the overlapping areas in three montages of serial sections, n, $n + 1$, and $n + 3$. The cytoplasmic invagination, as well as heterochromatin masses in the nucleus and mitochondria in the cytoplasm, can be used as guiding markers to locate an area within the nucleus in serial sections. The montages were composed of three to eight aerial photographs enlarged from negatives taken at a magnification of ×23,000.

Immunoelectron microscopy. For immunoelectron microscopy, the monolayers were fixed with a combination of 1% water-soluble 1-ethyl-3(3-dimethylaminopropyl) carbodiimide (Sigma, St. Louis, Mo.) and 0.2% glutaraldehyde as previously described (19). They were permeabilized either in 0.05% saponin or in 0.1% Nonidet P-40 in 10 mM Tris-HCl (pH 7.0)–150 mM NaCl–2 mM ethylene glycol-bis(β-aminoethyl ether)-*N,N,N',N'*-tetraacetic acid (EGTA) for at least 1 h at 37°C with gentle agitation and treated sequentially with goat IgG (1 mg/ml) for 2 h, affinity-purified rabbit anti-Vp1 IgG (20 μg/ml) for 2 h, and 5-nm colloidal gold particle (CGP)-conjugated goat anti-rabbit IgG (Ted Pella, Inc., Redding, Calif.) diluted 1:20 in 0.1% cold-water-fish gelatin (Sigma) for 2 h. All antibody dilutions, incubations, and intervening wash steps were carried out with the above-described saponin solution at 37°C. Excess reagent was washed away after each incubation with three changes, 30 min each, of saponin solution at 37°C. Following the last incubation and wash, samples were fixed in 2.5% glutaraldehyde in PBS and then processed for EM as described above.

RESULTS

Nuclear accumulation of the protein component of SV40 is arrested by chilling and metabolic energy depletion. Nuclear transport of NLS-harboring proteins through NPCs has been shown to be arrested by chilling and to require metabolic energy (7, 39). To test whether the nuclear targeting of SV40 is also arrested at a low temperature, we examined the subcellular localization of viral proteins Vp1 and Vp3 in virion-injected cells at 37°C and at 0 to 4°C. As expected, at 37°C, Vp1 and Vp3 localized to the nucleus within 2 h postinjection (Fig. 1A and B). In contrast, when precooled cells were injected with SV40 and subsequently maintained on ice for an additional 2 h, the nuclear accumulation of both proteins was arrested and the proteins remained in the cytoplasm (Fig. 1C and D). In these cells, perinuclear rim staining of Vp1 was observed (Fig. 1G and H). The perinuclear staining was similar to that observed in nucleoplasmin- and histone H1-injected cells at a low temperature (7, 39). The chilling effect was reversible; when virion-injected cells that had been incubated at 4°C before and after injection were shifted to 37°C for 1 h before fixation, both proteins localized to the nucleus (Fig. 1E and F).

We next examined the requirement of metabolic energy for the nuclear targeting of SV40. In the presence of normal levels of glucose in Eagle's basal medium, Vp1 and Vp3 localized to the nucleus 2 h after microinjection (data not shown). When the cells were depleted of energy by treatment with sodium azide and 2-deoxyglucose (see Materials and Methods), both proteins remained in the cytoplasm at 2 h postinjection (data not shown; their protein localization patterns were identical to those shown in Fig. 1C and D). When the microinjected, energy-depleted cells were transferred to normal glucose-containing medium, both proteins localized to the nucleus 1 h after the medium change (data not shown), indicating the reversibility of the inhibition. The temperature as well as energy dependency of the nuclear accumulation of SV40 proteins supports our conclusion that NPCs are a route of nuclear entry for microinjected SV40 virion proteins.

SV40 entry into the nuclei of nonpermissive cells. To test whether SV40 virions enter the nuclei of both nonpermissive and permissive cells by the same route, we injected virions into the cytoplasm of NIH 3T3 cells. Injected virion Vp1

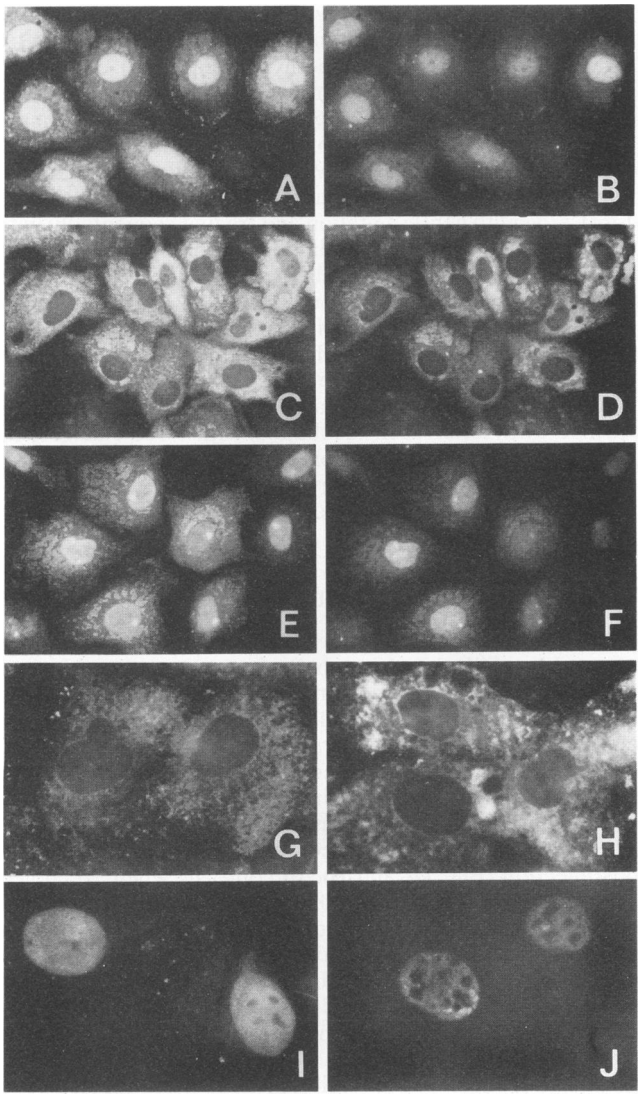

FIG. 1. Subcellular localization of Vp1, Vp3, and T antigen. (A through H) Effect of chilling on the nuclear accumulation of Vp1 and Vp3 in permissive TC7 cells. (I and J) Nuclear accumulation of Vp1 and large T antigen in nonpermissive NIH 3T3 cells. (A and B) Cells were incubated at 37°C for 2 h following cytoplasmic injection of SV40. (C and D) Precooled cells were cytoplasmically injected with virion particles and subsequently incubated for 2 h on ice before fixation. (E and F) Virion-injected cells that had been treated exactly as in panels C and D were shifted to 37°C for 1 h before fixation. For panels A through H, cells were reacted with guinea pig anti-Vp1 and rabbit anti-Vp3 antibodies and then with TRITC–goat anti-guinea pig and FITC–goat anti-rabbit antisera. (I and J) NIH 3T3 cells cytoplasmically injected with SV40 were cultured for 2 h (I) or 4 h (J), fixed, and reacted with rabbit anti-Vp1 (I) or hamster anti-large-T-antigen (J) antisera and then with TRITC–goat anti-rabbit IgG (I) or FITC-goat anti-hamster IgG (J). (A, C, E, G, H, and I) Anti-Vp1 antibody staining. (B, D, and F) Anti-Vp3 antibody staining. (J) Anti-T-antigen antibody staining. (G and H) Higher magnifications of cells treated as in panel C. The perinuclear binding of Vp1 is visible.

localized to the nucleus within 2 h of cytoplasmic injection (Fig. 1I), and nuclear large T antigen was observed 4 h postinjection or 2 h after nuclear Vp1 accumulation (Fig. 1J). As in permissive TC7 cells, the nuclear import of Vp1 in NIH 3T3 cells was arrested by chilling or in the presence of antinucleoporin antibody (data not shown). Thus, the ability to use NPCs appears to be a general property of the microinjected virus.

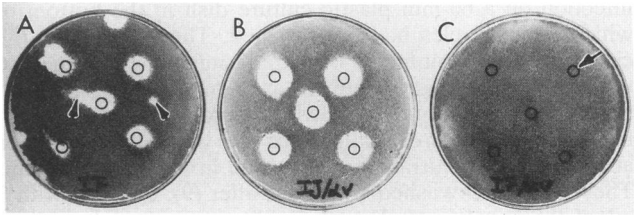

FIG. 2. Ability of injected and infected SV40 to form plaques. Cells inside marked circles (e.g., arrow in C) were microinfected with SV40 in the presence (C) or absence (A) of SV40-neutralizing antibody or cytoplasmically microinjected with virions in the presence of the neutralizing antibody (B). Cells were cultured in semisolid agar medium for 14 days, fixed, and then stained with crystal violet. Irregularly shaped plaques that had not been aimed for microinfection are indicated by arrowheads in A and were presumably due to virions that leaked from the capillary during infection.

Ability of cytoplasmically injected SV40 to complete the infectious cycle and propagate. To further substantiate the idea that cytoplasmically injected virions are able to complete the viral lytic cycle and propagate, we performed a plaque formation assay (Fig. 2). About 100 cells in medium containing virus-neutralizing antibody were cytoplasmically injected with SV40 particles and allowed to propagate in semisolid agar medium for 14 days, at which time the presence of plaques was assayed. As a control, plaque formation following viral infection was assayed by microinfecting cells in the absence or presence of the virus-neutralizing antibody. In the SV40-injected cultures, clearly round-shaped plaques were seen around and concentric to the microinjected area (Fig. 2B), while in SV40-infected cultures, round-shaped plaques were also seen around the microinfected area, but the plaques were irregular and smaller in size than those resulting from microinjection (Fig. 2A). As anticipated, the presence of the neutralizing antibody prevented plaque formation by microinfected virus (Fig. 2C) and assured that the cell surface-mediated infection, if any, due to leaked virus during the cytoplasmic injection was blocked effectively (9). These results demonstrate that cytoplasmically injected SV40 particles are capable of completing the infectious cycle, leading to secondary infection and forming plaques.

Time-dependent interference with nuclear T-antigen accumulation by mAb414 following SV40 infection. For papovavirus infection, virion particles are internalized, following adsorption, into the cytoplasm after being enveloped by the plasma membrane (22, 23, 25, 30, 32, 35). We thus wished to assess the route of nuclear entry for virions that are introduced by infection rather than injection. It should be noted that the subcellular localization of Vp1 after microinfection could not be monitored cytochemically, presumably because of low levels of virion internalization. We thus monitored infection by determining nuclear large-T-antigen accumulation. The accumulation of nuclear large T antigen in the early phase of virus infection occurs about 10 to 12 h after the adsorption of virions to cells and is a result of serial events, including internalization, intracytoplasmic trafficking, virion nuclear entry, expression of the gene, and nuclear targeting of the gene product. While the first two events are unique to

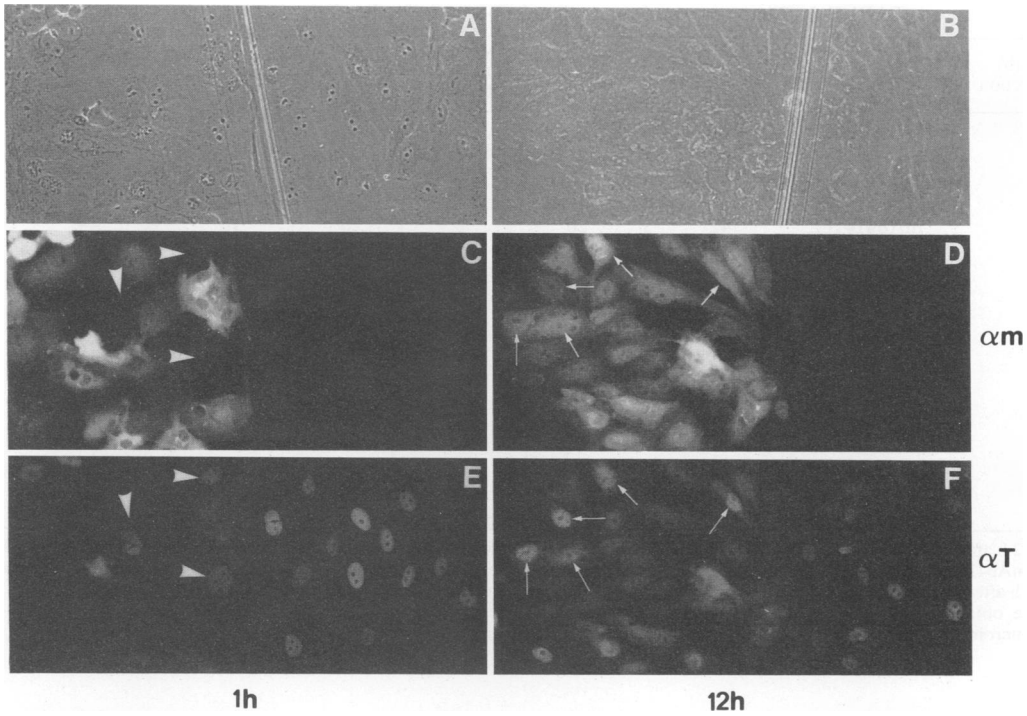

FIG. 3. Effect of mAb414 on virion infection. Cells on both sides of a diamond pen-etched line (shown in panels A and B) were microinfected with SV40. At 1 (A, C, and E) or 12 (B, D, and F) h after infection, mAb414 was cytoplasmically injected into the cells on the left side of the line. At 20 h after viral infection, cells were fixed, reacted with TRITC–goat anti-mouse IgG (αm) and hamster anti-large-T-antigen (αT) antisera, and then reacted with FITC–goat anti-hamster IgG. (C and E) The mAb414-injected cells shown in panel C were devoid of the nuclear large-T-antigen staining shown in panel E, except for three cells (arrowheads) that escaped mAb414. Nuclear large-T-antigen staining is indicated by arrowheads in panel E. (D and F) Arrows indicate cells that accumulated nuclear large T antigen and were injected with mAb414.

the infection, the last three events commence in both infected and cytoplasmically virion-injected cells. The time required for the last three in injected cells has been estimated to be 3 to 4 h (9). The time required for nuclear T-antigen accumulation did not change when a few virions, 10 to 100, instead of 1,000 to 10,000, were cytoplasmically injected (data not shown). If the infecting virions enter through the NPCs, nuclear T-antigen accumulation is expected to be inhibited by the cytoplasmic injection of antinucleoporin antibody after infection within a finite time period. Once the early gene is expressed following virion nuclear entry and its gene product accumulates in the nucleus of infected cells, the reagent should interfere only with the subsequent nuclear import of the gene product. The finite time period should allow us to evaluate the unique phase of the infection.

The effect of a transport inhibitor on the nuclear accumulation of large T antigen was examined following SV40 microinfection (Fig. 3; Table 1). At 1, 4, 8, or 12 h after SV40 infection, mAb414 was injected cytoplasmically into cells, such as those shown to the left of the line in Fig. 3A and B. Similarly, a mouse anti-human kappa-chain-constant-region antibody, Idh 3.3.6, was cytoplasmically injected 1 h after virus infection as a control. The subcellular localizations of mouse IgG (mAb414 and Idh 3.3.6) and large T antigen were determined 20 h after infection by indirect double-immunofluorescence microscopy. Cell viability did not suffer appreciably up to 24 h after cytoplasmic injection of either antibody (data not shown). When mAb414 was injected 1 h after infection, large T antigen was not observed in mAb414-injected cells (Fig. 3C and E; Table 1) but was seen in the nuclei of uninjected cells (to the right of the line in Fig. 3E; Table 1). Cells that escaped the mAb414 injection showed nuclear large-T-antigen staining (indicated by arrowheads in Fig. 3C and E; Table 1). A similar observation was made when the reagent was injected into the infected cells 4 or 8 h postinfection (Table 1). Cytoplasmic injection of Idh 3.3.6 did not affect the nuclear accumulation of large T antigen (Table 1), indicating that the lack of large-T-antigen expression in the above-described mAb414-injected cells was specific to the action of the antinucleoporin antibody. In contrast, when mAb414 was delivered 12 h after infection, the reagent had very little effect on nuclear large-T-antigen accumulation; even in the antibody-injected cells, nuclear staining of large T antigen was seen (indicated by arrows in Fig. 3D and F; Table 1). The nuclear accumulation of large T antigen in those cells must have occurred before the injection of mAb414. These results indicate that the blockade by the antinucleoporin antibody of nuclear T-antigen accumulation following SV40 infection is time dependent, occurs for up to 8 h of infection, and succumbs to the action of the reagent once virions are imported into the nucleus anytime during the subsequent 4 h (8 to 12 h of infection). These results also suggest that the process that includes internalization and intracytoplasmic trafficking is slow and takes at least 8 h during an infection.

Ultrastructural observations. (i) Subcellular distribution of electron-dense particles in virion-injected cells. To refine our previous ultrastructural observations that the majority of cytoplasmically injected SV40 virion particles are imported to the nucleus shortly after injection, we processed cells

TABLE 1. Time course of the antinucleoporin antibody effect on SV40 infection[a]

Expt	Time (h) postinfection	Cytoplasmic injection	No. of cells examined	No. of cells that were				No. of cells examined	No. of cells that were T^+
				$T^-/m\alpha^+$	$T^-/m\alpha^-$	$T^+/m\alpha^+$	$T^+/m\alpha^-$		
1	1	None	—	—	—	—	—	55	41
		Idh 3.3.6	47	0	2	36	9	—	—
2	1	None	—	—	—	—	—	48	39
		mAb414	42	26	2	0	14	—	—
3	1	None	—	—	—	—	—	48	38
		mAb414	53	39	3	0	11	—	—
2	4	None	—	—	—	—	—	41	30
		mAb414	48	31	6	0	11	—	—
2	8	None	—	—	—	—	—	49	36
		mAb414	41	32	0	0	9	—	—
4	12	None	—	—	—	—	—	56	36
		mAb414	50	37	0	11	2	—	—

[a] At 1, 4, 8, or 12 h after SV40 microinfection, cells in half of a designated area were cytoplasmically microinjected with either mouse anti-human antibody Idh 3.3.6 or antibody mAb414, while cells in the other half received no injection (none), as described in Materials and Methods and in the legend to Fig. 3. The cells were harvested 20 h after infection. The number of cells in the area was obtained from phase-contrast micrographs, and the $T^-/m\alpha^+$, $T^-/m\alpha^-$, $T^+/m\alpha^+$, $T^+/m\alpha^-$, and T^+ cells were obtained from immunofluorescence micrographs (T represents T antigen, and mα represents mouse antibodies). —, not determined. Experiments for microinfection and microinjection were performed as sets.

fixed 1.5 h after microinjection for EM. In agreement with our previous observations, many spherical electron-dense particles (Fig. 4A, B, and C, arrows) were seen in the nuclei. Such electron-dense particles are tentatively designated virion particles. Virion particles were distributed randomly but nonuniformly in the nucleoplasm but not in heterochromatin or in nucleoli (data not shown). The average diameter of the particles in the nucleoplasm was 38.2 ± 4.3 nm (n = 100). An average of 2.5 virion particles per μm^2 per section were counted, amounting to 10.3 particles per μm^3, in the nucleoplasm. If a volume of about 700 μm^3 is assumed for the 23.2- and 4.64-μm oblate ellipsoid TC7 cell nucleus (18), the number of virion particles in one nucleus, as estimated from those found in the nucleoplasm of serial sections, is about 7×10^3 (see Materials and Methods). Virion particles were absent in the cytoplasm as well as in organelles, such as mitochondria, the endoplasmic reticulum, and the Golgi apparatus (Fig. 4A and B). In the control noninjected cells, spherical electron-dense particles were seen neither in the nuclei (Fig. 4D) nor in the cytoplasm.

Tangential cross sections of NPCs were also visualized. An area(s) bisected by the nuclear envelope and showing distinct double nuclear membranes, such as those seen in Fig. 4A and B, contained many donut-shaped NPCs (Fig. 4C and D). They were interspersed with the nuclear matrix. The average outer diameter, inner diameter, nearest NPC-NPC distance, and density of NPCs were estimated to be 85.3 ± 8.6 nm (n = 100), 40.2 ± 8.5 nm (n = 100), 208.2 ± 67.7 nm (n = 100), and 12.5 ± 2.9 pores per μm^2, respectively.

(ii) Virion particles in NPCs. We have shown that virion particles are seen predominantly in the cytoplasm and in the vicinity of NPCs of mAb414-coinjected cells (9). Transport arrest provided an opportunity to observe virion particles in the NPCs (Fig. 5). In transport-arrested cells, virion particles were seen near the inner nuclear membrane (Fig. 5A, arrows only, and 5C, short arrows), intersecting the nuclear envelope (Fig. 5A, arrow with arrowhead, and 5B, arrow), and in the NPCs (Fig. 5C, long arrows, and 5E through I). In the tangential sections of the NPCs, electron-dense particles were seen inside and at the center of the donut-shaped NPCs of virion-injected cells (Fig. 5C, long arrows, and 5E through I). Such electron-dense particles were not observed in nonvirion-injected cells (Fig. 5D, arrowheads, and 5J through L). The average diameter of the two electron-dense particles appearing in each of the NPCs in Fig. 5C (long arrows) was 21.3 nm, and that in eight NPCs was 24.2 ± 6.9 nm, considerably smaller than the average diameter of virion particles seen in the nucleoplasm (see above).

(iii) Immunogold-Vp1 labeling of NPCs. To confirm that electron-dense particles observed near and in NPCs reflected SV40 particles, we performed immunoelectron microscopy with affinity-purified anti-Vp1 IgG and CGPs conjugated with the secondary antibody (Fig. 6). Although overall structural detail suffered from the permeabilization process, NPCs were seen as an amorphous mass intercepting the nuclear envelope but connecting fused outer and inner nuclear membranes in sections perpendicular or slightly oblique to the plane of the nuclear envelope (Fig. 6A, C, and F). Multiple CGPs were observed at the cytoplasmic entrance to NPCs (Fig. 6A and C, arrowheads), and two CGPs were seen in association with an NPC (Fig. 6F, arrowhead). In the tangential sections of the nuclear envelope, donut-shaped NPCs were visible (Fig. 6B, D, and E, arrowheads), although the poor morphology caused by detergent treatment made them less discernible from surrounding structures, such as those shown in the lower half of Fig. 6B. CGPs were either in the NPCs (Fig. 6B, D, and E, arrows, and Fig. 6I through M) or in the area with the poor structural detail (Fig. 6B, lower right).

The CGPs were rarely found in the cytoplasm or in the vicinity of the NPCs of virion-injected cells, in which the primary antibody treatment was omitted (data not shown), or were limited to the cell periphery and were rarely found in the vicinity of the NPCs of virion-infected cells (data not shown). The latter observation for the infected cells is in agreement with the lack of Vp1 staining observed for virion infection (see above). Since the CGPs decorating virions adsorbed to the cell surface of infected cells were readily

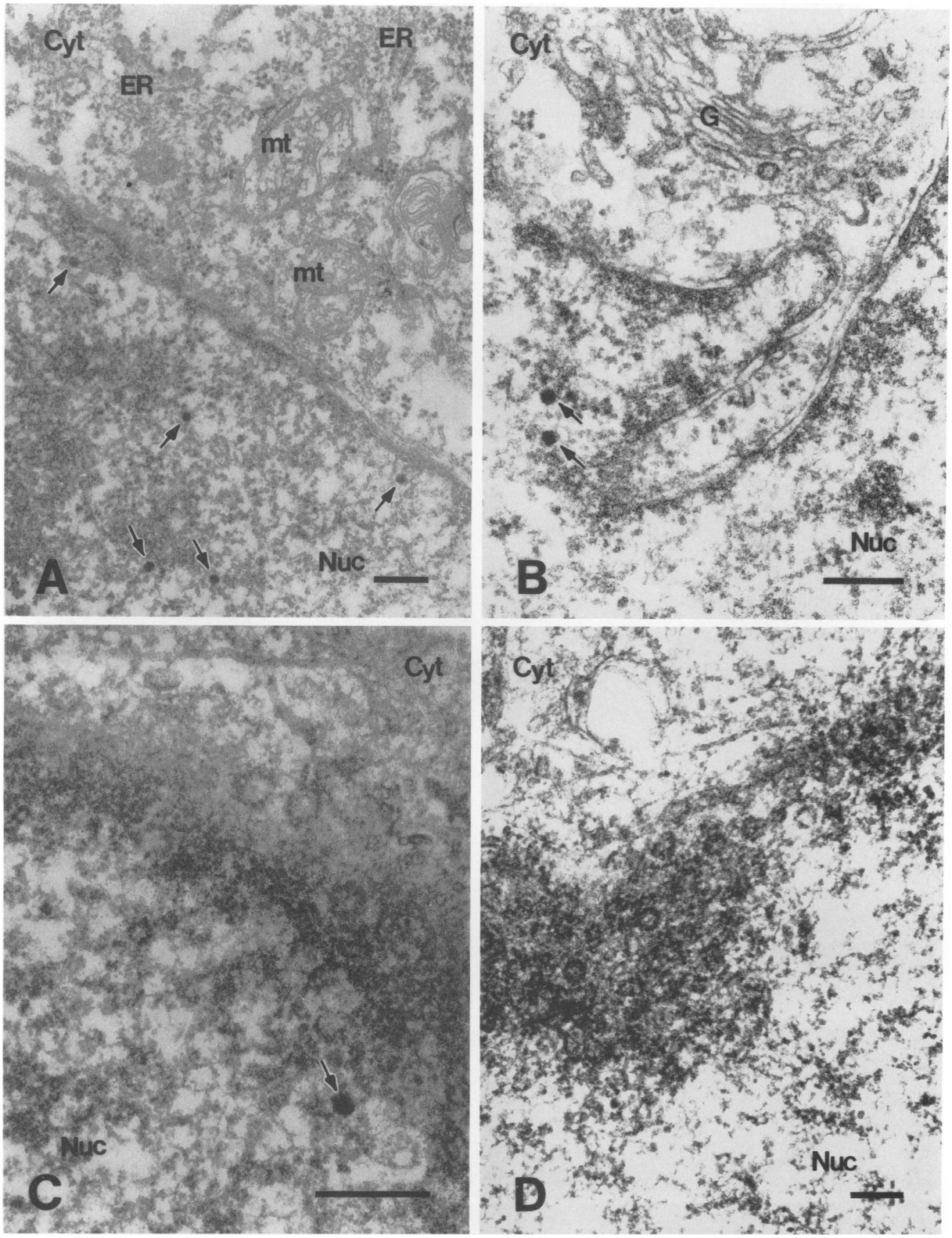

FIG. 4. Subcellular localization of cytoplasmically injected SV40. (A, B, and C) Electron micrographs of virion-injected cells. Cytoplasmically injected cells were incubated for 1.5 h prior to fixation. (D) Electron micrograph of noninjected control cells. Arrows indicate SV40 particles. mt, mitochondria; G, Golgi apparatus; ER, endoplasmic reticulum; Nuc, nucleoplasm; Cyt, cytoplasm. Bars, 200 nm. Tangential sections of NPCs are aligned in an orderly fashion among the nuclear matrices (C and D). The nearest NPC-NPC distance, 208.2 ± 67.7 nm (n = 100), was measured as the distance between the centers of two NPCs in an area containing a cluster of more than four NPCs. Twenty areas were selected for the measurement. The number of NPCs per square micrometer, 12.5 ± 2.9, was obtained by counting the NPCs in 30 different areas measuring 1 μm^2 each.

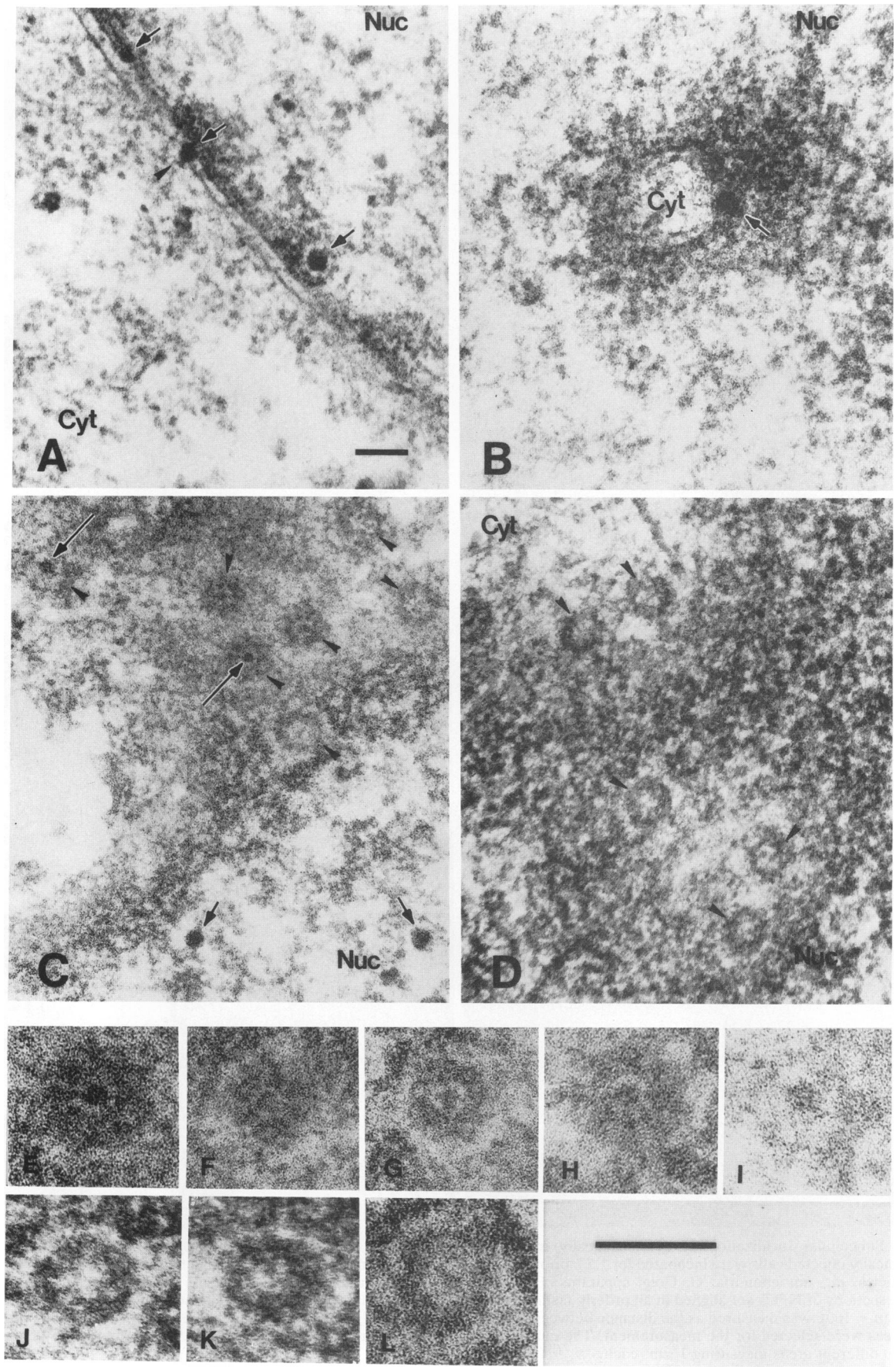
Nuc
Cyt
A
Nuc
Cyt
B
C
Nuc
Cyt
D
Nuc
E
F
G
H
I
J
K
L

visible (data not shown), fewer virions appeared to be internalized during infection.

For cell permeabilization, we used either saponin or Nonidet P-40. In either case, virion particles in the nucleoplasm of virion-injected samples, such as those shown in Fig. 4A and B, were not distinguished from the cell structure and were rarely decorated by the CGPs. A few clusters of CGPs were occasionally observed (Fig. 6G and H) but were insufficient to account for the number of virion particles observed in Fig. 4. This scarcity of CGP decoration of SV40 in the nucleus could suggest that the diffusion into the nucleus of the immunoreagents, anti-Vp1 antibody and 5-nm CGP-coated IgG, was ineffective or that the antigenic determinants in the nucleus were inaccessible to the reagents. Nonetheless, the immunogold-Vp1 labeling of NPCs provides evidence that the morphologically observed electron-dense particles contained the viral structural proteins.

DISCUSSION

We have now shown that the nuclear import of SV40 proteins derived from cytoplasmically injected virions is arrested at a low temperature and when cells are energy depleted. This nuclear transport arrest further corroborates our previous observation that the nuclear entry of SV40 is blocked in the presence of NPC-inhibitory reagents (9). The ability to use NPCs as an entrance to the nucleus is a general property of the cytoplasmically introduced virus, since the nuclear accumulation of both viral protein and large T antigen in nonpermissive NIH 3T3 cells was quite similar to that in permissive TC7 cells. Using a plaque assay, we have shown that cytoplasmically injected SV40 is able to reproduce and propagate. Since infection by virions exuded from the needle during the injection was not eliminated in reported experiments (20), an assay for virion propagation 48 h after cytoplasmic injection could include virions resulting from virus infection in addition to those resulting from injection. With inclusion of the SV40-neutralizing antibody during injection, the ambiguity has now been clarified. The cytoplasmic introduction of mAb414 effectively blocked nuclear T-antigen accumulation for up to 8 h of infection but had very little effect after 12 h of infection. Ultrastructural studies have revealed SV40 virion particles in the nucleoplasm, near the heterochromatic region, near the inner nuclear membrane, intersecting the nuclear envelope, and in the NPCs of cells. The presence of virion particles in the latter two regions was enhanced in transport-arrested cells. NPCs and adjacent areas were selectively decorated by anti-Vp1 IgG–CGPs, indicating that electron-dense particles observed in the NPCs contained viral structural proteins.

The experimental evidence presented here indicates that cytoplasmically introduced SV40 particles enter the nucleus through NPCs in a manner analogous to the nuclear transport of NLS-containing karyophilic proteins, as has been shown in in vitro and in vivo import experiments (7, 13, 33, 34, 39). ATP has been shown to be required for the translocation of signal-containing proteins through NPCs (24, 33, 34, 39); however, whether it is required for the nuclear import of SV40 particles is not yet known. While it is consistent with our data that this ATP requirement is related to the NPC-mediated translocation process, the transport arrest observed when cells were energy depleted or chilled could have been due to the inhibition of an earlier, prerequisite step in the cytoplasm. The microinjection approach would not distinguish between inhibition at the nuclear transport step and that at this putative earlier step. Since the presence of the electron-dense particles in NPCs was enhanced in transport-arrested cells, our inhibition results are consistent with our interpretation that the block is at the nuclear transport step. The nuclear uptake of SV40 would thus be receptor mediated, analogous to that shown for NLS-harboring proteins (1, 21, 40, 43, 45).

The pore complex subunits that comprise the octagonal symmetry (2, 4, 38, 42) were rarely visualized but more often were not resolved, presumably because of the thickness of the specimen preparation. The average outer diameter of the dehydrated TC7 cell NPCs (85.3 ± 8.6 nm), as determined by a surface view of an NPC by thin sectioning after osmium tetroxide fixation, compares reasonably well with that reported for vertical sections of 3T3-L1 cells (12). This value for TC7 cells is smaller than that reported for amphibian oocytes in dehydrated specimens (17, 38, 42) or in specimens flash frozen in liquid nitrogen (2, 38). NPCs are considered to be randomly scattered over the nuclear surface, and this irregularity, together with the topological irregularity inherent to sectioning of cells, appears to have had an effect on the nearest NPC-NPC distance. Nonetheless, the values for the nearest NPC-NPC distance and the NPC density, 208.2 ± 67.7 μm and 12.5 ± 2.9 pores per μm^2, respectively, are also in good agreement with reported values (31).

Feldherr and coworkers (10, 13) have shown that NPCs appear able to transport large nucleoplasmin-coated CGPs up to 26 nm in diameter. Akey (3), using functional binding site mapping studies (4), recently proposed a double-iris model for passage of the NLS-containing protein molecules. According to the model, nuclear proteins first bind to the periphery of the transporter and then move and dock to the transporter prior to translocation through the NPCs. The size of an intact virion (approximately 50 nm) is much larger

FIG. 5. SV40 in NPCs. mAb414-coinjected and incubated cells (A, B, and C) or noninjected cells (D) were processed for EM as described in Materials and Methods. (A) Cross section revealing a double nuclear envelope. Two virion particles (arrows only) are just inside the inner nuclear membrane, and one particle (arrow with arrowhead) is in an NPC. The nucleus (Nuc) and the cytoplasmic side (Cyt) are marked. (B) Cross section of a cytoplasmic invagination (Cyt) in the nucleus (Nuc). A particle (arrow) intercepts the nuclear envelope. (C) An area of the nucleus (Nuc) showing donut-shaped NPCs (arrowheads). Two NPCs contain electron-dense particles (long arrows) in the center of the pores. On the basis of the overall structure adjacent to the photo shown, the cytoplasm is situated beyond the top and the nucleoplasm is situated beyond the bottom of the photograph. A mesh-like network invades most of the lower right area, suggesting that this area is just inside the inner nuclear membrane. The two virion particles seen at the bottom (short arrows) are probably on the inner nuclear membrane side of the NPCs. (D) Cross section of the NPCs of control cells. Arrowheads show NPCs. (E through I) Enlarged images of NPCs, each showing an electron-dense virion in the center. (J through L) NPCs without particles. Image L is from a transport-arrested sample, and images J and K are from panel D. The average diameters of virions in the NPCs and of free virions in the nucleoplasm were measured in eight NPCs like those marked by long arrows in panel C and in 100 virions like those marked by short arrows in the nucleoplasm in Fig. 4A and panel C. In some areas in panel D, the NPCs contained, in the center, a very small electron-dense spot whose diameter was 9.7 ± 2.1 nm (n = 8), while a majority of the NPCs were devoid of a spot. Such a spot, presumably a central plug, was distinctly smaller than average virions seen in the NPCs in panel C. Bars, 100 nm.

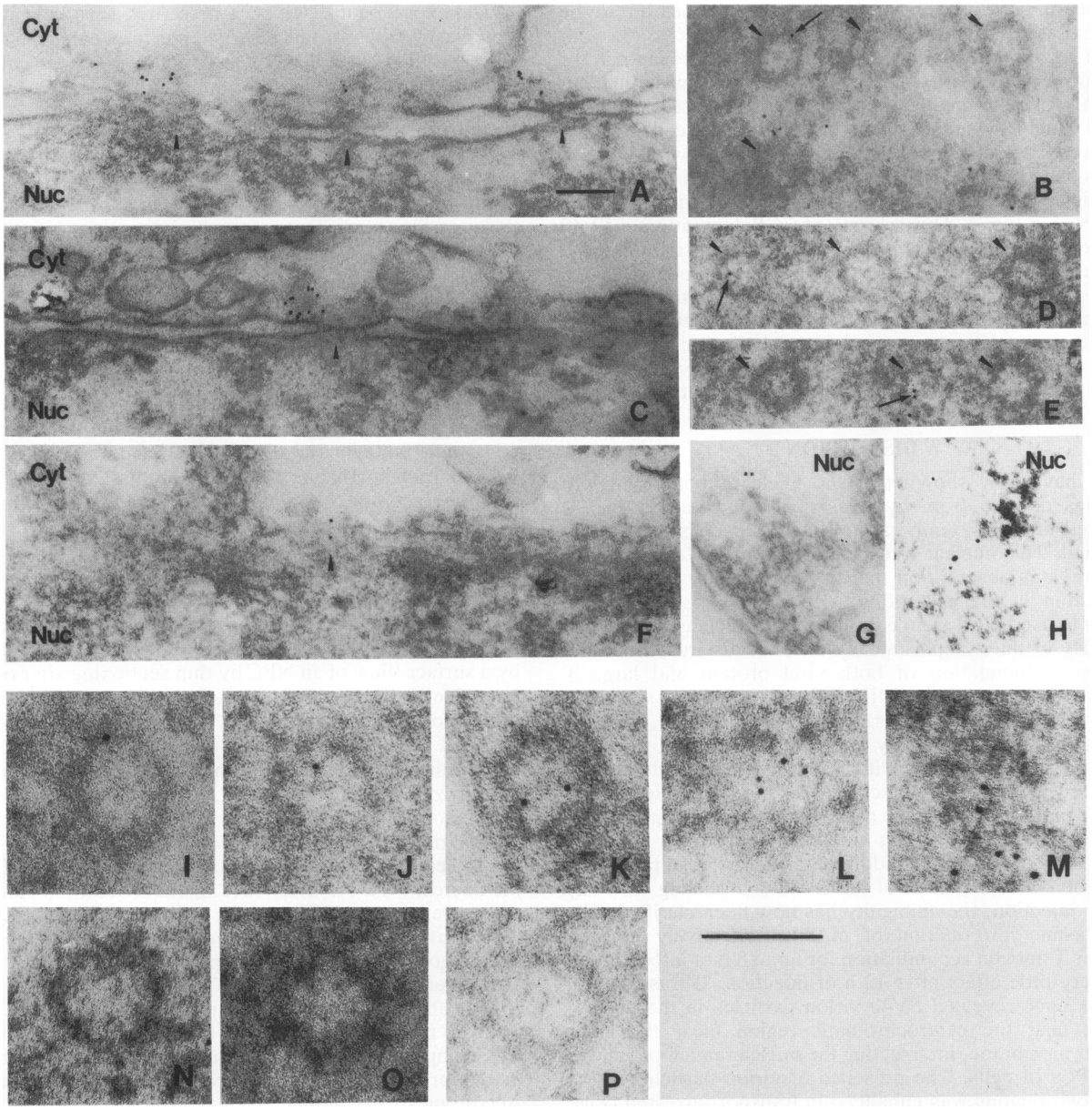

FIG. 6. Immunoelectron micrographs of SV40-injected cells. Cells were prepared for immunoelectron microscopy as described in Materials and Methods. Saponin was used for permeabilization. Arrowheads indicate NPCs, and arrows indicate 5-nm CGPs in donut-shaped NPCs. Nuc, nucleoplasm; Cyt, cytoplasm. Bars, 100 nm. (A and C) Vertical sections of nuclear envelopes showing the multiple CGPs on the cytoplasmic side (Cyt) of all NPCs. (F) Vertical but oblique section showing two gold particles in association with an NPC. (B, D, and E) Tangential sections of nuclear envelopes showing donut-shaped NPCs and CGPs in NPCs (arrows) or in the vicinity of NPCs. (G and H) CGPs in the nucleoplasm (Nuc). The virion particles in the nucleus of virion-injected cells were rarely labeled with CGPs. Poor labeling was also observed in cells permeabilized with Nonidet P-40. (I through M) Enlarged images showing 5-nm CGPs in NPCs. NPCs with CGPs were selected from those surrounded by more than a few discernible NPC structures. (N through P) Enlarged images of NPCs devoid of CGPs.

than the proposed opening size of the transporter (up to 26 nm) in the double-iris model (3). In this study, we observed size differences of ca. 10 nm between the diameters of electron-dense particles in the nucleoplasm (38.2 ± 4.3 nm) and in the NPCs (24.2 ± 6.9 nm). The latter diameter is substantially larger than that reported for the central plug (3, 4, 17, 42). It should be noted that the diameter in the NPCs was measured from NPC samples showing distinctive electron-dense particles in the center. For example, an electron-dense particle (Fig. 5E) was distinguished from the surroundings because of the presence, within the donut-shaped structure (with average outer and inner diameters of 85.3 ± 8.6 and 40.2 ± 8.5 nm, respectively), of a concentric space that permitted an electron beam. A dense mass occluding the NPC would have been less apparent. Thus, the actual size difference could be smaller than the presented value, and the observation could be interpreted as an intact virion capable of passing through an NPC; the NPC, in response to a large NLS-harboring macromolecule, could undergo a structural alteration that has yet to be discovered. Alternatively, the

size difference could implicate a partial dissociation of the virion particles as they go through the NPCs, and the observed particles could be dissociated but subassembled structures that may or may not be devoid of viral DNAs. Further studies must address the possible molecular mechanism of the nuclear entry of SV40 virions through NPCs.

The data shown for the time-dependent interference with nuclear T-antigen accumulation following SV40 infection by the antinucleoporin antibody are consistent with our hypothesis that the infecting virions also enter the nucleus through NPCs. This hypothesis is further supported by our recent results, in which nuclear T-antigen accumulation was prevented in SV40-infected cells by the cytoplasmic injection of anti-Vp1 or anti-Vp3 IgG (42a). We showed here that mAb414-injected cells survived the long incubation period and were viable, as has been shown for another monoclonal antinucleoporin antibody, RL-1 (11). Although PtK2 cells microinjected with mAb414 cannot go through the telophase of the cell cycle (5), the telophase transition should not pose a problem for our analysis, as infected cells are arrested at the interphase (41). The results, however, are compounded by the general inhibitory nature of the antibody; we do not know whether mAb414 blocked virion nuclear entry, the subsequent nuclear entry of large T antigen, or a combination of both. Until we develop a means to selectively and directly block the nuclear entry of infecting virions, the question of whether infecting virus enter the nucleus through NPCs remains unsolved. Identification of the virion NLS supposedly exposed at the surface of virions, as well as the study of mutant virions for infection, should contribute to the understanding of the role of NPCs in viral reproduction.

An intriguing observation was that nuclear large-T-antigen accumulation could be interrupted for up to 8 h of infection. The following 4 h were sufficient to target to the nucleus both infecting virions and the subsequently expressed gene product. The time required for virion nuclear entry followed by T-antigen expression in the infected cells is in good agreement with that observed for cytoplasmically injected virions (9). The fact that there was very little change in the time required for nuclear T-antigen accumulation when a few virions instead of a large number were cytoplasmically injected indicates that virion copy number has very little to do with the time required for the detection of the gene product once virions reach NPCs and additionally supports the presence of a well-coordinated step that leads to gene expression. It further implies that the early stage of virus infection consists of two steps: a slow intracytoplasmic trafficking step including the virus internalization process and a relatively fast nuclear entry step. What would slow intracytoplasmic trafficking of endocytosed virions? First, selection at the cell surface could lower the number of virions entering cells; not all virions at the cell surface can be endocytosed during viral infection, as has been corroborated in this study as the lack of the detection of Vp1 staining as well as anti-Vp1 IgG-CGP in the cytoplasm of infected cells. With fewer available infectious particles, any obstacle would greatly lengthen the time required to reach the nucleus. Second, during infection, plasma membranes enclosing endocytosed virions fuse with organelle membranes (23, 25, 30, 32), and this fusion process may entrap virions in the organelles, reducing the pool of virions enroute to the nucleus. This interpretation is opposite to the role of the membrane transport pathway proposed previously for viral infection (23, 25, 30, 32). In contrast to the reported observations, we rarely observed virion particles in the nuclear envelope or in the cytoplasmic organelles in the virion-injected cells. Even in the transport-arrested specimens, in which virion particles were abundant in the cytoplasm, few electron-dense particles were found (two particles in serial sections of 15 nuclei) in the intracisternal space of the nuclear envelope or in cytoplasmic organelles. Contrary to this scarcity of particles in the envelope, electron-dense particles were relatively easy to detect in NPCs of the transport-arrested virion-injected cells. If the virion NLS plays a role in virion particle passage through an NPC, endocytosed or organelle-bound virions would have to be released from these compartments to expose the NLS, thus delaying the time to reach the reproductive site, or would remain permanently trapped in these compartments, reducing the number of particles targeted to the nucleus. We believe that virion particles do not have a selective mechanism for avoiding entrapment by membraneous organelles and therefore go through an ineffective and lengthy intracytoplasmic trafficking process during viral infection.

ACKNOWLEDGMENTS

We are grateful to S. Morrison and L. Wims for the gift of Idh 3.3.6; J.-P. Revel for the use of a Philips 420 EM; R. Consigli, D. Dean, and D. Goldfarb for comments and critical reading of the manuscript; R. Consigli, M. Fried, and G. Warren for stimulating discussions; and D. Dean and J. Clever for advice and criticism. We also thank J. Clever for assistance in the NIH 3T3 transport arrest study.

This work was supported by Public Health Service grant CA 50574 and by a grant from the University of California, Los Angeles, Academic Senate.

REFERENCES

1. **Adam, S. A., T. J. Lobi, M. A. Mitchell, and L. Gerace.** 1989. Identification of specific binding proteins for a nuclear location sequence. Nature (London) **337**:276–279.
2. **Akey, C. W.** 1989. Interactions and structure of the nuclear pore complex revealed by cryo-electron microscopy. J. Cell Biol. **109**:955–970.
3. **Akey, C. W.** 1990. Visualization of transport-related configurations of the nuclear pore transporter. Biophys. J. **58**:341–355.
4. **Akey, C. W., and D. S. Goldfarb.** 1989. Protein import through the nuclear pore complex is a multi-step process. J. Cell Biol. **109**:971–982.
5. **Benevente, R., U. Scheer, and N. Chaly.** 1989. Nucleocytoplasmic sorting of macromolecules following mitosis: fate of nuclear constituents after inhibition of pore complex function. Eur. J. Cell Biol. **50**:209–219.
6. **Bonner, W. M.** 1975. Protein migration into nuclei. I. Frog oocyte nuclei in vivo accumulate microinjected histones, allow entry to small proteins, and exclude large proteins. J. Cell Biol. **64**:421–430.
7. **Breeuwer, M., and D. S. Goldfarb.** 1990. Facilitated nuclear transport of histone H1 and other small nucleophilic proteins. Cell **60**:999–1008.
8. **Clever, J., and H. Kasamatsu.** 1991. Simian virus 40 Vp2/3 small structural proteins harbor their own nuclear transport signal. Virology **181**:78–90.
9. **Clever, J., M. Yamada, and H. Kasamatsu.** 1991. Import of simian virus 40 virions through nuclear pore complexes. Proc. Natl. Acad. Sci. USA **88**:7333–7337.
10. **Dworetzky, S. I., R. E. Lanford, and C. M. Feldherr.** 1988. The effects of variations in the number and sequence of targeting signals on nuclear uptake. J. Cell Biol. **107**:1279–1287.
11. **Featherstone, C., M. K. Darby, and L. Gerace.** 1988. A monoclonal antibody against the nuclear pore complex inhibits nucleocytoplasmic transport of protein and RNA in vivo. J. Cell Biol. **107**:1289–1297.
12. **Feldherr, C. M., and D. Akin.** 1990. The permeability of the nuclear envelope in dividing and nondividing cell cultures. J. Cell Biol. **111**:1–8.

13. **Feldherr, C. M., E. Kallenbach, and N. Schultz.** 1984. Movement of a karyophilic protein through the nuclear pores of oocytes. J. Cell Biol. **99**:2216–2222.
14. **Fendrick, J. L., and L. M. Hallick.** 1983. Optimal conditions for titration of SV40 by the plaque assay method. J. Virol. Methods **7**:93–102.
15. **Fields, B. N., D. M. Knipe, R. M. Chanock, M. S. Hirsch, J. L. Melnick, T. P. Monath, and B. Roizman (ed.).** 1990. Virology. Raven Press, New York.
16. **Finlay, D. R., D. D. Newmeyer, T. M. Price, and D. J. Forbes.** 1987. Inhibition of in vitro nuclear transport by a lectin that binds to nuclear pores. J. Cell Biol. **104**:189–200.
17. **Franke, W. W.** 1974. Structure, biochemistry and functions of the nuclear envelope. Int. Rev. Cytol. **4**(Suppl.):71–236.
18. **Fung, B.** 1984. Ph.D. thesis. University of California, Los Angeles.
19. **Fung, B. P., and H. Kasamatsu.** 1985. Immuno-electron-microscopic localization of a centriole-related antigen in ciliated cells. Cell Tissue Res. **239**:43–50.
20. **Gershey, E. L., and E. G. Diacumakos.** 1978. Simian virus 40 production after viral uncoating in the CV-1 cell nucleus. J. Virol. **28**:415–416.
21. **Goldfarb, D. S., J. Gariepy, G. Schoolnik, and R. D. Kornberg.** 1986. Synthetic peptides as nuclear localization signals. Nature (London) **322**:641–644.
22. **Griffith, G. R., S. J. Marriott, D. A. Rintoul, and R. A. Consigli.** 1988. Early events in polyomavirus infection: fusion of monopinocytotic vesicles containing virions with mouse kidney cell nuclei. Virus Res. **10**:41–52.
23. **Hummeler, K., N. Tomassini, and F. Sokol.** 1970. Morphological aspects of the uptake of simian virus 40 by permissive cells. J. Virol. **6**:87–93.
24. **Imamoto-Sonobe, N., Y. Yoneda, R. Iwamoto, H. Sugawa, and T. Uchida.** 1988. ATP-dependent association of nuclear proteins with isolated rat liver nuclei. Proc. Natl. Acad. Sci. USA **85**:3426–3430.
25. **Kartenbeck, J., H. Stukenbrok, and A. Helenius.** 1989. Endocytosis of simian virus 40 into the endoplasmic reticulum. J. Cell Biol. **109**:2721–2729.
26. **Kasamatsu, H., and M. Wu.** 1976. Protein-SV40 DNA complex stable in high salt and sodium dodecyl sulfate. Biochem. Biophys. Res. Commun. **68**:927–936.
27. **Lanford, R. E., P. Kanda, and R. C. Kennedy.** 1986. Induction of nuclear transport with a synthetic peptide homologous to the SV40 T antigen transport signal. Cell **46**:575–582.
28. **Lang, I., M. Scholz, and R. Peters.** 1986. Molecular mobility and nucleocytoplasmic flux in hepatoma cells. J. Cell Biol. **102**: 1183–1190.
29. **Lin, W., T. Hata, and H. Kasamatsu.** 1984. Subcellular distribution of viral structural proteins during simian virus 40 infection. J. Virol. **50**:363–371.
30. **MacKay, R. L., and R. A. Consigli.** 1976. Early events in polyoma virus infection: attachment, penetration, and nuclear entry. J. Virol. **19**:620–636.
31. **Maul, G. G., J. W. Price, and M. W. Lieberman.** 1971. Formation and distribution of nuclear pore complexes in interphase. J. Cell Biol. **51**:405–418.
32. **Maul, G. G., G. Rovera, A. Vorbrodt, and J. Abramczuk.** 1978. Membrane fusion as a mechanism of simian virus 40 entry into different cellular compartments. J. Virol. **28**:936–944.
33. **Newmeyer, D. D., and D. J. Forbes.** 1988. Nuclear import can be separated into distinct steps in vitro: nuclear pore binding and translocation. Cell **52**:641–653.
34. **Newmeyer, D. D., J. M. Lucocq, T. R. Burglin, and E. M. De Robertis.** 1986. Assembly in vitro of nuclei active in nuclear protein transport: ATP is required for nucleoplasmin accumulation. EMBO J. **5**:501–510.
35. **Nishimura, T., N. Kawai, M. Kawai, K. Notake, and I. Ichihara.** 1986. Fusion of SV40-induced endocytic vacuoles with the nuclear membrane. Cell Struct. Funct. **11**:135–141.
36. **Paine, P. L., and S. B. Horowitz.** 1980. The movement of material between nucleus and cytoplasm. Cell Biol. **4**:299–338.
37. **Paine, P. L., L. C. Moore, and S. B. Horowitz.** 1975. Nuclear envelope permeability. Nature (London) **254**:109–114.
38. **Reichelt, R., A. Holzenburg, E. L. Buhle, Jr., M. Jarnik, A. Engel, and U. Aebi.** 1990. Correlation between structure and mass distribution of the nuclear pore complex and of distinct pore complex components. J. Cell Biol. **110**:883–894.
39. **Richardson, W. D., A. D. Mills, S. M. Dilworth, R. A. Laskey, and C. Dingwall.** 1988. Nuclear protein migration involves two steps: rapid binding at the nuclear envelope followed by slower translocation through nuclear pores. Cell **52**:655–664.
40. **Silver, P., I. Sadler, and M. Osborne.** 1989. Yeast proteins that recognize nuclear localization sequences. J. Cell Biol. **109**:983–989.
41. **Tooze, J. (ed.).** 1981. DNA tumor viruses. Cold Spring Harbor Laboratory, Cold Spring Harbor, N.Y.
42. **Unwin, P. N. T., and R. A. Milligan.** 1982. A large particle associated with the perimeter of the nuclear pore complex. J. Cell Biol. **93**:63–75.

42a. **Yamada, M.** Unpublished data.

43. **Yamasaki, L., P. Kanda, and R. E. Lanford.** 1989. Identification of four nuclear transport signal-binding proteins that interact with diverse transport signals. Mol. Cell Biol. **9**:3028–3036.
44. **Yoneda, Y., T. Arioka, N. Imamoto-Sonobe, H. Sugawa, Y. Shimonishi, and T. Uchida.** 1987. Synthetic peptides containing a region of SV40 large T-antigen involved in nuclear localization direct the transport of proteins into the nucleus. Exp. Cell Res. **170**:439–452.
45. **Yoneda, Y., N. Imamoto-Sonobe, Y. Matsuoka, R. Imamoto, Y. Kiho, and T. Uchida.** 1988. Antibodies to Asp-Asp-Glu-Asp can inhibit transport of nuclear proteins into the nucleus. Science **242**:276–278.